Inorganic Chemistry

Article

pubs.acs.org/IC

Extremely Long Cu···O Contact as a Possible Pathway for Magnetic Interactions in $Na_2Cu(CO_3)_2$

Yulia V. Nelyubina,* Alexander A. Korlyukov, Ivan V. Fedyanin, and Konstantin A. Lyssenko

A.N. Nesmeyanov Institute of Organoelement Compounds, Russian Academy of Sciences, Vavilova Str., 28, 119991 Moscow, Russia

Supporting Information

ABSTRACT: Chemical binding in a mixed copper sodium carbonate $Na_2Cu(CO_3)_2$, a layered material showing ferromagnetic intralayer exchange and weak antiferromagnetic interlayer coupling, was examined within the topological analysis of experimental (from high-resolution X-ray diffraction) and theoretical (from periodic quantum chemical calculations) electron density functions in its crystal. Together with modeling of a superexchange pathway within the LSDA and DFT+U approach, the results obtained reveal a very weak Cu···O interaction (0.5 kcal/mol worth) between the copper–carbonate layers that is nevertheless stabilizing (bonding) and may serve as a possible pathway for antiferromagnetic interactions.

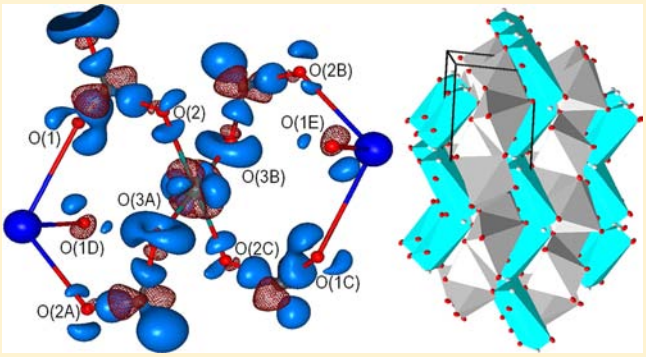

INTRODUCTION

Magnetic properties are among the most important and intriguing properties of crystalline solids,[1] making them of practical use in many different fields of our everyday life.[2] Many efforts have been made to rationalize magnetic behavior of chemical substances (from metal salts[1] to purely molecular compounds[3]); all efforts have been made to more deeply understand and control it.[2] The latter challenges those specializing in design of new magnetic materials to constantly search for the relations of magnetic properties and structural peculiarities, as their main tools are to specifically design a certain binding motif[4] or to use an interplay of noncovalent interactions.[5] Both these strategies are based on the knowledge of chemical interactions that govern the arrangement of magnetic centers in a particular crystal.

Among the most powerful approaches to identify and quantify chemical interactions is an analysis of electron density distribution, obtained either from high-resolution X-ray diffraction data or periodic quantum chemical calculations, within *R.* Bader's "Atoms in Molecules" theory.[6] It provides accurate information on all bonding interactions in a crystal, which are identified by a presence of bond critical points (bcps)[6] and quantified on the basis of a value of local potential energy $v(r)$[7] therein through the Espinosa's correlation that was initially proposed for H bonds[8,9] and then transferred to other types of interatomic interactions.[10] Although shown to be a useful tool for defining possible magnetic interaction pathways through weak intermolecular interactions in crystals,[11,12] its use for this purpose was limited to evaluating 3D orbital populations of a metal atom and locating a bcp between metal centers.[12−15] If there were no such bcps (sometimes even if there was one[16]), the magnetic interaction was assumed to occur through a superexchange mediated by bridging ligands.

To check if the topological analysis of an electron density distribution can do more than that, we have chosen sodium bis(carbonato)cuprate(II),[17] which occurs in nature as the mineral juangodoyite.[18] The most intriguing feature of this crystalline material is its magnetic behavior as a 3D antiferromagnet that is closely related to its structural peculiarities.[19] The crystal structure of $Na_2Cu(CO_3)_2$ consists of successive layers $[Cu(CO_3)_2^{2-}]$ with the copper atoms in a nearly ideal square-planar environment that are coupled ferromagnetically but also display weak antiferromagnetic interlayer interactions.[19] The latter was suggested to be the result of direct exchange between the copper atoms from the neighboring layers (they are, however, 5.6 Å apart) or a superexchange via the sodium ions that are between them.

So the question arises, is there some sort of a bonding interaction between sodium and copper cations in $Na_2Cu(CO_3)_2$, or are they bound through carbonate species only? The latter option may also explain weak antiferromagnetic coupling between the layers, as there was one example reported of similar interactions mediated by a long M−O−Na−O−M superexchange path in $NaNiO_2$.[20] A possibility for a supposed binding mode of copper to be [4 + 2] should also be examined, as ferromagnetic and antiferromagnetic coupling is possible through carbonate anions,[19,21,22] and here the coordination sphere of copper may be extended by including "apical" oxygen atoms located at 2.7591(8)−3.5808(8) Å (Figure 1), some of them from the neighboring layers. Close contacts between

Received: September 23, 2013
Published: November 22, 2013

   dx.doi.org/10.1021/ic4024025 | *Inorg. Chem.* 2013, 52, 14355−14363

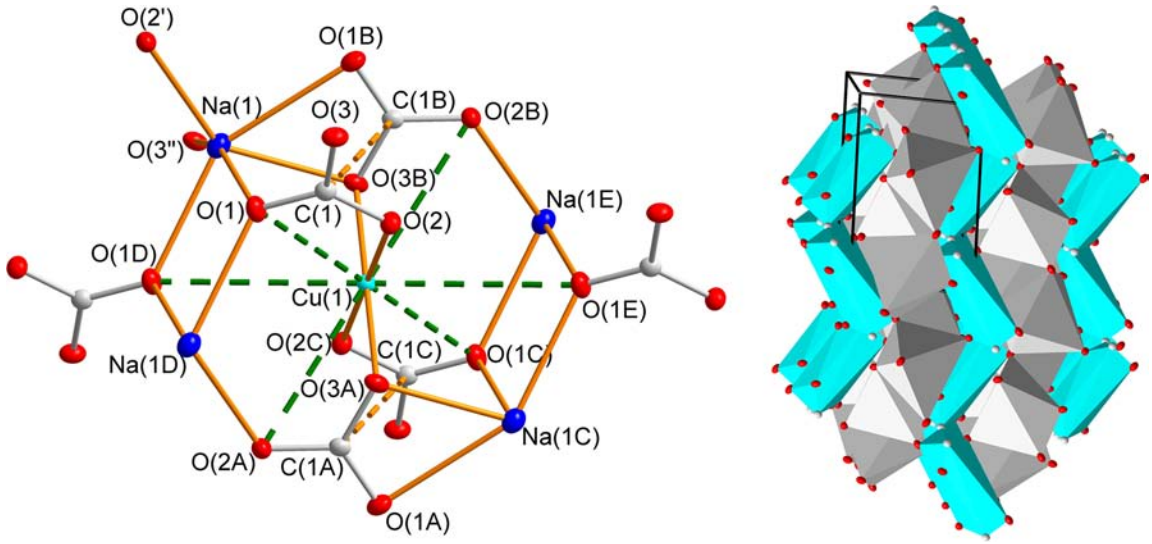

Figure 1. General view of $Na_2Cu(CO_3)_2$ in a crystal from X-ray diffraction data: (left) in the representation of atoms by thermal ellipsoids (p = 80%) showing the coordination environment of copper and sodium atoms as well as one of the anion−anion shortened contacts; (right) in the representation of copper and sodium atoms as coordination polyhedra showing copper−carbonate layers (in cyan). The interatomic distances (Å) for given bonds and interactions are: Na(1)−O(1) 2.4315(8), Na(1)−O(1B) 2.6512(9), Na(1)−O(1D) 2.5010(9), Na(1)−O(2′) 2.3148(8), Na(1)−O(3B) 2.4150(9), Na(1)−O(3″) 2.3901(8), Cu(1)−O(2) 1.9313(7), Cu(1)−O(3A) 1.9446(7), Cu(1)···O(1) 2.7591(8), Cu(1)···O(1D) 3.5808(8), Cu···O(2A) 3.2871(8), C(1)···C(1B) 3.086(1).

carbonate species may additionally help hold the layers together, although the shortest occurs within them, rather than between them.

Enhanced insight into these aspects of $Na_2Cu(CO_3)_2$ has been obtained with the topological analysis of an electron density function $\rho(\mathbf{r})$, obtained both experimentally from X-ray diffraction data and theoretically from quantum chemical calculations, within *R.* Bader's "Atoms in Molecules" theory.[6] Note that an early electron density investigation of $Na_2Cu(CO_3)_2$[17] did not go beyond qualitative description of the deformation electron density within the closest coordination environment of the copper atom, although revealing the importance of second-nearest-neighbor interactions.

EXPERIMENTAL METHODS AND THEORETICAL CALCULATIONS

Crystals of $Na_2Cu(CO_3)_2$ (M = 229.54) are monoclinic, space group $P2_1/c$, at 120K: a = 5.6327(4), b = 8.1237(6), c = 6.1520(5) Å, β = 115.8051(12)°, V = 253.43(3) Å^3, Z = 2 (Z' = 1/2), d_{calc} = 3.008 gcm^{-3}, μ (Mo Kα) = 44.43 cm^{-1}, F(000) = 222. Intensities of 9301 reflections were measured with a Bruker SMART 1000 CCD diffractometer [λ (Mo Kα) = 0.71072 Å, ω-scans, 2θ<105°], and 2928 independent reflections [R_{int} = 0.0347] were used in further refinement. These data were collected in three batches, a low-angle (2θ = −32°), a middle-angle (2θ = −62°), and a high-angle batch (2θ = −92°), in an omega-scan mode ($\Delta\omega$ = 0.5°) with a detector to a sample distance of 4.1 cm at exposure times of 4 s for the low-angle reflections, 8 s for the middle-angle reflections, and 12 s for the high-angle reflections, respectively, to yield a high-resolution data set (sinθ/λ up to 1.1 Å^{-1}). Raw data were integrated by using the program SAINT and then scaled, merged, and corrected for Lorentz-polarization effects using the SADABS package.[23] Semiempirical absorption correction from equivalents was applied using SADABS.

The structure was solved by the direct method and refined by the full-matrix least-squares technique against F^2 in the anisotropic approximation. The refinement converged to wR2 = 0.0726 and GOF = 1.007 for all the independent reflections (R1 = 0.0305 was calculated against F for 2290 observed reflections with $I > 2\sigma(I)$). All calculations were performed using SHELXTL PLUS 5.0 software.[24] CSD 426576 contains the supporting crystallographic data for this paper. These data can be obtained free of charge from Fachinformationszentrum Karlsruhe, 76344 Eggenstein-Leopoldshafen, Germany (e-mail: crysdata@fiz-karlsruhe.de, http://www.fiz-karlsruhe.de/ecid/Internet/en/DB/icsd/depot_anforderung.html).

The multipole refinement against experimental structure factors was carried out within the Hansen−Coppens formalism[25] using the XD program package[26] with the core and valence electron density derived from the wave functions fitted to a relativistic Dirac−Fock solution.[27] Within the XD refinement, the 4s orbital of the copper atom was included in the "core" (to give a default [Ar]4s^1 neutral atom configuration) in agreement with the convention adopted for all other transition metals. Such a treatment of Cu(II) ion was, among others, preferred over other possibilities in a charge density study by L.J. Farrugia et al.[14] The level of multipole expansion was hexadecapole for copper and octupole for carbon and oxygen atoms; the monopole term was refined for all atoms. The refinement was carried out against F and converged to R = 0.0220, R_w = 0.0162 and GOF = 0.86 for 1749 merged reflections with $I > 3\sigma(I)$). The refinement of atomic coordinates and anisotropic displacement parameters (ADPs) was preformed against high-angle data (sinθ/λ = 0.7−1.1 Å^{-1}), and the refinement of all other parameters was performed up to sinθ/λ = 1.0 Å^{-1}. At the beginning, coordinates + ADPs were refined to obtained accurate positional coordinates and thermal parameters for all atoms, followed with the refinement of multipoles; both steps were repeated until R stops decreasing. Then, we introduced monopoles, first-order kappas and second-order kappas, all preceded and followed by coordinates + ADPs and multipoles refinement cycle, until repeating of any of these steps stop leading to deviation from obtained parameters and/or decrease of R. All covalently bonded pairs of atoms satisfy the Hirshfeld rigid-bond criteria;[28] the difference of the mean-square displacement amplitudes along the bonds being not larger than 6×10^{-4} Å^2. The results of data collection, spherical and multipole refinement against experimental structure factors for $Na_2Cu(CO_3)_2$ are listed in Table 1.

Theoretical structure factors were calculated within the periodical DFT approach with atom-centered Gaussian-type function basis sets as implemented in the Crystal09 software package.[29] We have used the combination of B3LYP functional[30] with TZVP basis set specially fitted for solid-state calculations.[31] Wave function was optimized in the experimental geometry, and then structure factors were calculated for

dx.doi.org/10.1021/ic4024025 | Inorg. Chem. 2013, 52, 14355−14363

Table 1. Details of Data Collection, Spherical and Multipole Refinement against Experimental Structure Factors for $Na_2Cu(CO_3)_2$

compound formula	$Na_2Cu(CO_3)_2$
compound color	blue
M	229.54
T	120K
space group	$P2_1/c$
crystal system	monoclinic
a, Å	5.6327(4)
b, Å	8.1237(6)
c, Å	6.1520(5)
β,°	115.8051(12)
V, Å^3	253.43(3)
Z	2
density, g·cm^{-3}	3.008
F(000)	222
μ (Mo K$_\alpha$), cm^{-1}	44.43
crystal size, mm	0.10 × 0.10 × 0.25
scan technique	ω-scan with 0.5° step in ω
absorption correction (Mo Kα)	semiempirical from equivalents
θ_{max}, °	52.5
no. of measured reflns	9301
no. of independent reflns (R(int))	2928 (0.0347)
no. of observed reflns with $I > 2\sigma(I)$	2290
spherical refinement	
wR2	0.0726
R1 calculated against F	0.0305
GOF	1.007
ρmax/ρmin, eÅ^{-3}	1.394/−1.142
multipole refinement	
no. of rfln. with $I > 3\sigma(I)$	1749
R1 calculated against F	0.0220
R_w calculated against F	0.0162
GOF	0.86
ρmax/ρmin, eÅ^{-3}	0.259/−0.240

5898 independent reflections up to the resolution d = 0.355 Å (sinθ/λ up to 1.419 Å^{-1}). Multipole refinement against theoretical structure factors was performed in static model, by using XD program package (with the same sinθ/λ cutoffs as used for the refinement against experimental structure factors).[26] The refinement was carried out against F and converged to R = 0.0060 and GOF = 0.12 for 2126 reflections.

In both cases, the total electron density function was positive everywhere, with the largest residual electron density as low as 0.26 eÅ^{-3} located in the vicinity of the Na(1) atom's nucleus; the corresponding minimum near the Cu(1) atom being −0.24 eÅ^{-3}. Analysis of the topology of the resulting $\rho(r)$ functions was carried out using the WINXPRO program package.[32]

The potential energy density $v(r)$ was evaluated through the Kirzhnits's approximation[33] for the kinetic energy density function $g(r)$. Accordingly, the $g(r)$ function is described as $(3/10)(3\pi^2)^{2/3}[\rho(r)]^{5/3} + (1/72)|\nabla\rho(r)|^2/\rho(r) + 1/6\nabla^2\rho(r)$, leading in conjunction with the local virial theorem $(2g(r) + v(r) = 1/4\nabla^2\rho(r))$ to the expression for $v(r)$ and making it possible to estimate the electron energy density $h_e(r)$.

The interaction energies were estimated by means of the Espinosa's correlation scheme—a semiquantitative relation between the energy of an interaction and the value of the potential energy density function $v(r)$ in its bcp.[8,9] Having a very simple form as 0.5 $v(r)$, it was repeatedly shown to give accurate estimates in many cases (those are succinctly summarized in ref 10), including weak interactions such as H···H and C−H···O,[34] Mg···C and Ca···C interactions,[35,36] strong and intermediate hydrogen bonds,[37] Ca−O(carbonate),[38] Au−PPh$_3$ and Gd−OH$_2$ bonds,[39,40] which belong to the intermediate type of intermolecular interactions,[6] and so forth. The interaction energies thus obtained were shown to accurately reproduce the energy of a crystal lattice;[34,38,41,42] the discrepancy between the crystal lattice energies estimated in such a manner from X-ray diffraction data and those measured experimentally can be as small as 0.2 kcal/mol.[34,43] The latter value, divided by a number of interactions used to obtain the sublimation enthalpy by this approach, may be thought of as uncertainty in the interaction energies estimated by Espinosa's correlation, thus being of ∼0.02 kcal/mol.

Magnetic properties of $Na_2Cu(CO_3)_2$ were calculated using the VASP 5.3.3 program.[44−47] To describe valence electrons, a plane wave expansion was applied with a kinetic energy cutoff of 700 eV; core electrons were accounted by using PAW potentials.[48,49] Brillouin zone integration was carried out using 4 × 4 × 4 k-point set. All calculations were performed within the generalized gradient approximation (exchange−correlation functional PBE).[50,51] Coordinates of atoms and cell vectors of $Na_2Cu(CO_3)_2$ were optimized using the conjugated gradient technique, and the obtained structure served as a starting model for successive LSDA and DFT+U calculations. Initial magnetic moment was associated with copper atoms only and chosen as 2 μ_B. These calculations were performed for an optimized structure of $Na_2Cu(CO_3)_2$ and a 2 × 1 × 1 supercell. Electron densities obtained from nonspin-polarized calculations as well as LSDA and DFT+U were presented in numerical form as an equidistant 3D array. Distance between the points in the 3D array was equal to 0.0245 Å. The following topological analysis of numerical electron densities was carried out by the AIM program, which is a part of the ABINIT program package.[52]

RESULTS AND DISCUSSION

According to our high-resolution X-ray diffraction data for $Na_2Cu(CO_3)_2$, its molecular geometry and crystal packing are as described earlier:[17] low-symmetry carbonate anions (C−O 1.2607(10), 1.2951(10), and 1.3126(10) Å) are bound to copper atoms (which occupy special positions, an inversion center), thus forming copper−carbonate layers (Cu−O 1.9315(7) and 1.9450(6) Å) with sodium cations in between (Na−O 2.3142(8)−2.9087(10) Å). The smallest Cu···Cu separation in a crystal is 5.0953(6) Å; so, there is hardly any direct overlap of the coppers' 3d-orbitals, and all magnetic interactions should thus occur through a superexchange pathway involving carbonate and/or sodium ions.

Geometrical parameters of interionic contacts in $Na_2Cu(CO_3)_2$ also suggest the presence of a short Cu···Na contact (3.3572(5) Å) and additional long Cu···O interactions (see Figure 1) within the layers (Cu(1)···O(1) 2.7591(8) and Cu(1)···O(2A) 3.2871(8) Å) and between them (Cu(1)···O(1D) 3.5808(8) Å). To judge if there are indeed any of these interactions, we performed a search for the bcps of the experimental electron density function obtained from the X-ray diffraction data.

Its results revealed very little contribution from interactions between like-charged species, as is usually the case. In particular, there was no bcp for Na···Cu bonding, and only two bcps for weak anion−anion interactions (O···O 3.025(1) and 3.265(1) Å, see Table 2) were located between the layers (all visualized by bcps and bond paths). Note that bulky copper atoms do not allow the shortest anion−anion interaction to occur (Figure 1), as the corresponding bcp can only be found if copper cations are excluded from consideration.

Cation−anion interactions in a crystal of $Na_2Cu(CO_3)_2$ include six Na−O bonds with the interatomic distance of 2.3142(8)−2.6511(8) Å and six Cu−O interactions; those involve four oxygen atoms (O(2), O(2C), O(3A), and O(3B)) forming its square-planar environment and two distant oxygens

dx.doi.org/10.1021/ic4024025 | Inorg. Chem. 2013, 52, 14355−14363

Table 2. Interatomic Distances and Topological Parameters of $\rho(r)$ in bcps for All the Interionic Interactions in $Na_2Cu(CO_3)_2$ Derived from Experimental (First Line) and Theoretical (Second Line) Structure Factors

interaction[a]	n[b]	R, Å	$\rho(r)$, eÅ^{-3}	$\nabla^2\rho(\mathbf{r})$, eÅ^{-5}	$-v(r)$, au	$h_e(\mathbf{r})$, au	E_{int}, kcal/mol
Cu(1)−O(2)	2	1.9313(7)	0.63	11.47	0.1497	−0.0154	47.0
		1.9315	0.59	11.22	0.1380	−0.0108	43.3
Cu(1)−O(3A)	2	1.9446(7)	0.60	11.18	0.1416	−0.0128	44.4
		1.9445	0.57	10.52	0.1284	−0.0097	40.3
Cu(1)···O(1D)	2	3.5808(8)	0.03	0.22	0.0014	0.0005	0.4
		3.5810	0.03	0.21	0.0013	0.0004	0.4
Na(1)−O(2′)	1	2.3148(8)	0.12	3.18	0.0182	0.0074	5.7
		2.3142	0.12	3.10	0.0174	0.0074	5.5
Na(1)−O(3″)	1	2.3901(8)	0.10	2.49	0.0137	0.0061	4.3
		2.3896	0.09	2.33	0.0125	0.0059	3.9
Na(1)−O(3B)	1	2.4150(9)	0.10	2.42	0.0132	0.0059	4.2
		2.4148	0.10	2.45	0.0133	0.0060	4.2
Na(1)−O(1)	1	2.4315(8)	0.09	2.24	0.0123	0.0055	3.8
		2.4317	0.09	2.12	0.0115	0.0053	3.6
Na(1)−O(1D)	1	2.5010(9)	0.08	1.80	0.0094	0.0046	3.0
		2.5012	0.07	1.73	0.0090	0.0045	2.8
Na(1)−O(1B)	1	2.6512(9)	0.05	1.19	0.0057	0.0034	1.8
		2.6513	0.05	1.19	0.0057	0.0033	1.8
O(1)···O(1B)	1	3.025(1)	0.04	0.61	0.0034	0.0015	1.1
		3.025	0.05	0.60	0.0034	0.0014	1.1
O(3)···O(3′″)	1	3.265(1)	0.03	0.44	0.0022	0.0012	0.7
		3.265	0.03	0.36	0.0020	0.0009	0.6

[a]Atoms labeled with A are obtained from the basic ones by symmetry operations $-x, y-0.5, -z-0.5$, those with B, C, D, and E by $x, -y+0.5, z+0.5$; $-x, -y, -z$; $-x+1, -y, -z$ and $x-1, y, z$, respectively. Atoms labeled with asterisks are obtained from the basic ones by symmetry operations $x+1, -y+0.5, z+0.5$; $-x+1, y-0.5, -z+0.5$ and $-x+1, -y+1, -z$. [b]n stands for the number of interactions of this type the particular atom forms in a crystal.

O(1E) and O(1D). Although there are six additional oxygen atoms that can bind to copper (atoms O(1), O(1C), O(2A), and O(2B) in addition to O(1D) and O(1E) from Figure 1), only one set of bcps and bond paths was found, corresponding to the longest Cu···O(1D) and Cu···O(1E) interactions among all six of them (3.5808(8) Å). Note that other two long Cu···O contacts (Cu···O(1 and 1C) 2.7591(8) and Cu···O(2A and 2B) 3.2871(8) Å), which were not identified as stabilizing interactions, are observed within the layers, and the resulting bridging mode of carbonate species between the neighboring copper cations in a layer agrees with a ferromagnetic coupling therein.[21] For instance, if an interaction Cu(1)···O(1 or 1C) with an interatomic distance of 2.8 Å would occur, this binding mode will be the same as it was previously associated with an antiferromagnetic coupling.[21,53]

An identical set of interatomic interactions, including the above weak Cu···O binding, was also found in the electron distribution function obtained by multipole refinement against theoretical structure factors that were calculated within the periodical DFT approach; these results will be further used for comparison with those from high-resolution X-ray diffraction data.

Based on the topological parameters of the resulting experimental and theoretical electron densities in the relevant bcps (Table 2), the Na−O bonds correspond to the closed-shell type of interatomic interactions, with positive values of $\nabla^2\rho(r)$ and $h_e(r)$[54] ($h_e(r)$ being electron energy density) in the ranges of 1.19−3.18 eÅ^{-5} and 0.0033−0.0074 au. Their energy, which was estimated through the Espinosa's correlation[8,9] as a half of $-v(r)$ value, goes rather smoothly from 1.8 to 5.7 kcal/mol with the decrease in the interatomic distance. The same was also observed for Ca−O bonds in $CaCO_3$, although their energy reached as high as 11.8 kcal/mol.[38]

The Cu−O bonds within the layers are much stronger. In particular, the negative values of $h_e(r)$ together with positive $\nabla^2\rho(r)$ values (agreeing with M−O bond lengths[55,56]) in their bcps identify them as corresponding to the intermediate type of interactions. If using the classification based on the ratio $|v(r)|/g(r)$,[57] these Cu−O bonds have significant covalent contribution compared to ionic Na−O: the corresponding ratios are 1.09−1.11 for Cu−O and 0.63−0.71 for Na−O. Their energy, exhibiting the largest discrepancy between the experimental and theoretical electron densities (although the agreement between the two sets of topological parameters is very good overall[14]), is 44.4−47.0 and 40.3−43.3 kcal/mol, respectively. Note that the C−O bonds show the expected features associated with the delocalization of electron density over the carbonate anion, such as two lone pair domains of deformation electron density around each oxygen atom and high absolute values of $\rho(r)$, $\nabla^2\rho(r)$, and ellipticities at the bcps, which are equal to 0.90−1.15 eÅ^{-3}, −33.05 to −29.57 eÅ^{-5}, and 0.07−0.10, respectively, following the changes in the C−O bonds length (1.2607(10)−1.3126(10) Å). The $\nabla^2\rho(r)$ values as well as $h_e(r)$ therein (the latter being from −0.7473 to −0.6134 au) are negative, placing the C−O bonds into the shared-shell category. All these values are within the ranges previously found for $CaCO_3$[38] and azurite (a hydrated copper carbonate).[58]

Additional Cu···O bonds are more similar to anion−anion interactions in $Na_2Cu(CO_3)_2$. Both of them correspond to the closed-shell type of interactions, based on the $\nabla^2\rho(r)$ and $h_e(r)$ values as well as the ratio $|v(r)|/g(r)$; those are 0.2 eÅ^{-5}, 0.0005 au, 0.75, and 0.4−0.6 eÅ^{-5}, 0.0009−0.0015 au, 0.7 for Cu···O and O···O interactions, respectively. Note that these extremely

dx.doi.org/10.1021/ic4024025 | Inorg. Chem. 2013, 52, 14355−14363

long Cu···O bonds have slightly higher contribution of a shared character than Na−O bonds do. Their energy is estimated as 0.4 kcal/mol, similar to one obtained for the anion−anion interactions (0.7−1.1 kcal/kcal), which also happened to be weaker than in $CaCO_3$ (1.1−3.0 kcal/mol).[38] The latter is in line with the larger distance between interacting anionic species in $Na_2Cu(CO_3)_2$, although the presence of the copper atom was expected to significantly reduce their negative charges and thus to make their binding more efficient.

Indeed, the net charges of carbonate anions are −1.23 and −1.09 e, respectively, obtained by integrating $\rho(\boldsymbol{r})$ from the experimental and theoretical structure factors. For comparison, in $CaCO_3$ they were −1.45 and −1.49 e.[38] Such a difference is a result of strong Cu−O bonding in $Na_2Cu(CO_3)_2$ (with the total energy of 183.6 kcal/mol per one Cu cation), which causes a pronounced transfer of charge from carbonate to copper species with sodium cations participating to a small extent. In particular, upon the cation−anion binding in $Na_2Cu(CO_3)_2$, the sodium cation acquires ≈0.14 e, while the copper as much as 1.28 and 1.55 e (the latter difference in the values obtained in two ways is relatively small[14] and agrees with the corresponding discrepancies in the Cu−O bond energy). Note that the Cu(1) atomic charge of +0.72 e coincides nicely with that in azurite,[58] which was +0.71 and +0.74 e for two independent copper atoms in a unit cell, given the total energy of Cu−O bonds reaching 173 and 175 kcal/mol.[58]

In entirety, the atomic charges in $Na_2Cu(CO_3)_2$ estimated from both the experimental and theoretical structure factors agree rather well (Table 3); the lowest difference (∼0.01 e) is found for Na(1) while the highest (∼0.75 e) for C(1). The latter has been already observed for a sp^2 carbon in a zinc formate complex.[59]

Table 3. Experimental Atomic Charges and Volumes in a Crystal $Na_2Cu(CO_3)_2$ Derived from Experimental (First Line) and Theoretical (Second Line) Structure Factors[a]

atom	q, e	V_{at}, Å^3	atom	q, e	V_{at}, Å^3
Cu(1)	+0.72	12.88	O(1)	−1.25	16.39
	+0.45	13.25		−0.93	15.79
Na(1)	+0.87	9.20	O(2)	−1.14	14.32
	+0.86	9.50		−0.83	13.66
C(1)	+2.25	2.82	O(3)	−1.09	14.19
	+1.49	4.10		−0.82	13.71

[a]In both cases, the charge leakage was less than 0.01 e. The sum of atomic volumes (63.36 Å^3) reproduced well the volume of an independent part of the unit cell (63.36 Å^3) with a relative error of 0.002%. Although the integrated Langrangian ($L(r) = -1/4\nabla^2\rho(r)$) for every atomic basin has to be exactly zero, a reasonably small value averaging to 0.1 × 10^{-3} au was obtained.

All the topological and integrated parameters for $Na_2Cu(CO_3)_2$ are within the values reported in charge density studies of copper compounds, so there is no reason to suspect that weak Cu···O interactions found here are an artifact of experimental electron density distribution obtained from X-ray diffraction data or of the multipole model. In contrast, following the interpretation of bcps and associated bond paths as privileged exchange channels,[60] those for long Cu···O contacts provide experimental evidence for them being another probable superexchange pathway of antiferromagnetic coupling between the copper atoms in $Na_2Cu(CO_3)_2$.

Note that weak axial interactions Cu···O that may contribute to the magnetic behavior of a system were found in some copper(II) amino-propanolato complexes, but they were further ignored as displaying an unstable bonding graph.[14] In our case, however, the obtained molecular graph is very stable: all the corresponding bcps and bond paths were located in electron density obtained from experimental and theoretical structure factors within the multipole model with different refinement strategies employed and from quantum chemical calculations within the LSDA and DFT+U approach (see below).

Additional proof of the significance of these long Cu···O contacts for a magnetic behavior of $Na_2Cu(CO_3)_2$ comes from the deformation electron density around the copper atom and the related 3d-orbital occupancies (Table 4). The latter were estimated by means of orbital population analysis for transition metals proposed by Holladay et al.[61] valid in point group $\bar{1}$. As the copper site already has an inversion symmetry, no further restraints were applied; the shortest Cu−O bonds in a layer were chosen as x and y axis with z axis to its normal. The values thus obtained, all quite nicely reproducing those derived from charge density studies of complexes with a copper atom in an approximate D_{4h} environment (e.g., see refs 11,12,14,16), showed the partially occupied magnetic orbital to be $d_{x^2-y^2}$. Being an expected feature, it is clearly seen in the deformation electron density (DED) distribution around the copper atom as charge depletions facing oxygen atoms in a Cu−4O plane (Figure 2).

In a topological sense, these Cu−O bonds within a layer fall into a "peak-to-hole" type (Figure 3), complying with the "key-and-lock" rationalization provided for the bonding in coordination complexes.[62] Indeed, lone pair domains of the corresponding oxygen atoms O(2) and O(3) "look" toward the above depletions in a copper valence shell, so there is an efficient overlap with its magnetic orbital $d_{x^2-y^2}$. Among the second nearest neighbor oxygens, those at 2.7591(8) and 3.2871(8) Å from Cu(1) have their lone pair domains pointing at the charge concentration lobes of the copper atom (Figure 3B,C). Only the oxygen atom exhibiting bcp and bond path Cu···O(1) (3.5808(8) Å long) forms an interaction in the same "peak-to-hole" mode, as the closest to Cu(1) oxygen atoms do, and the bonding also involves copper's magnetic orbital $d_{x^2-y^2}$ (Figure 3B). One can see the lone pairs of the atom O(1D) or its symmetry equivalent atom O(1E), which are not exactly axial to the plane Cu−O4 (the tilt angle is 68.89(4)°), are directed to the corresponding lobes of the $d_{x^2-y^2}$ orbital of the copper atom.

Note that the charge accumulation domains of its most populated d_{z^2} orbital (see also Figure 1 of Supporting Information) are tilted toward the oxygen atoms O(1) and O(1C) at 2.7591(8) Å (the angle to the Cu−4O plane is 72° as

Table 4. 3d-Orbital Populations Derived from Experimental (First Line) And Theoretical (Second Line) Structure Factors

$d_{x^2-y^2}$	d_{z^2}	d_{xz}	d_{yz}	d_{xy}	total
1.50 (15.2%)	2.44 (24.8%)	1.90 (19.4%)	2.05 (20.8%)	1.95 (19.8%)	9.84
1.61 (15.9%)	2.08 (20.6%)	2.12 (21.0%)	2.13 (21.1%)	2.17 (21.4%)	10.10

dx.doi.org/10.1021/ic4024025 | Inorg. Chem. 2013, 52, 14355−14363

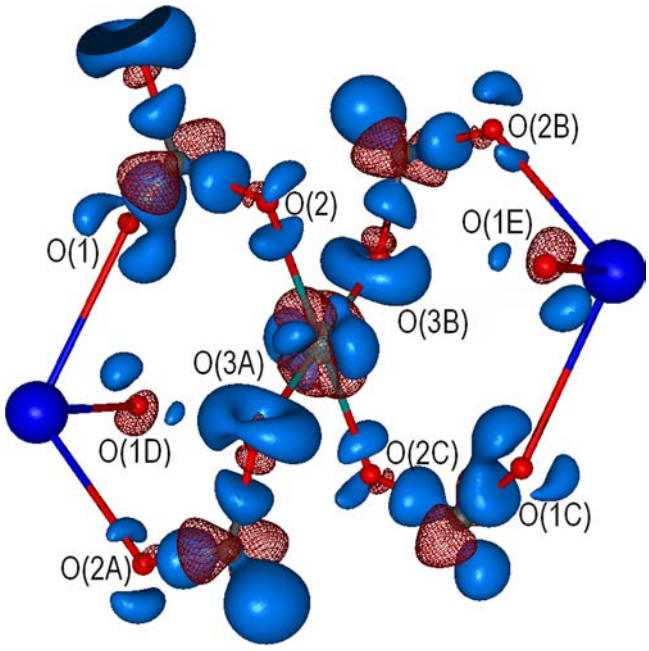

Figure 2. Three-dimensional distribution of the experimental DED around the copper atom from X-ray diffraction data. Isosurface of DED = 0.3 eÅ^{-3} shown by blue and with DED = −0.3 eÅ^{-3} by red wireframe. For labeling scheme, see caption to Figure 1 and footnote to Table 2.

judged by the positions of the highest maxima of $-\nabla^2\rho(\boldsymbol{r})$ in the copper's valence shell) allowing the atom O(1D) and O(1E) to access the charge density depletions attributed to the $d_{x^2-y^2}$ orbital (although one cannot exclude a strong interaction with the d_{z^2} orbital). This explains why there is a bonding interaction with the farthest oxygen atom from the augmented coordination sphere of copper and no bonding with two others, exactly as it was observed in the topological analysis. Moreover, this weak Cu···O interaction may occur as an overlap with the magnetic orbital of copper, supporting our assumption of its importance in the magnetic properties of $Na_2Cu(CO_3)_2$ as a possible mediator of superexchange.

Apart from bcp and bond path observed for this long Cu···O interaction in both the experimental and theoretical electron densities, there are some other pieces of evidence coming from quantum chemistry. Note that modeling of a superexchange pathway is still a challenge even in the case of a comparatively simple system, such as $Na_2Cu(CO_3)_2$. To date, there are two commonly accepted methods to treat spin-polarized systems: LSDA and DFT+U.

Prior to a spin-polarized calculation, atomic coordinates and cell vectors of $Na_2Cu(CO_3)_2$ were optimized. The use of a pure PBE functional led to the decrease in the unit cell volume by 7%; with a Grimme dispersion correction, it resulted in a more pronounced contraction (up to 11%), so the data from a calculation with the pure PBE functional were used in further discussion. This gave us an optimized structure with the geometrical parameters satisfactorily reproducing those from X-ray diffraction data: the bonds Cu−O within the layers varied by 0.01−0.02 Å and Cu···O between them by 0.06 Å. Despite these discrepancies, the optimization of $Na_2Cu(CO_3)_2$ was necessary to improve the convergence in spin-polarized calculations. Indeed, the use of experimental coordinates made convergence almost impossible in the case of DFT+U.

The LSDA and DFT+U calculations performed for a unit cell of $Na_2Cu(CO_3)_2$ yielded two types of solutions (ferromagnetic and antiferromagnetic). As the magnetic measurements of its crystals[19] showed the antiferromagnetic order to be aligned along the *a* axis of the unit cell, a 2 × 1 × 1 supercell was constructed to examine the antiferromagnetic behavior of $Na_2Cu(CO_3)_2$ in more detail. The symmetry of the resulting system was then switched off, so adjustment of a sign and a value of the initial magnetic moment was enough to obtain a target antiferromagnetic solution. Note that two such solutions were obtained in both the LSDA and DFT+U calculations (their energies differed by less than 0.001 eV), and only one of them had the same antiferromagnetic ordering as described earlier.[19]

Calculated at the LSDA level, the absolute value of magnetization at the copper atom is equal to 0.583 μ_B associated with its d-electrons; its d-orbital population is 8.835 e (Table 5). As was expected, the oxygen atoms O(2) and O(3) involved in the strong Cu−O bonding within the copper−carbonate layers exhibit nonzero values of magnetization (0.071 and 0.067 for the atoms O(2) and O(3), respectively), attributed mostly to their p-electrons. The magnetization of the atom O(1) bound to copper only through weak Cu···O interaction is much lower (0.011) but still nonzero, suggesting its involvement in superexchange, unlike the adjacent carbon atom or the sodium cation, which display zero magnetization. For comparison, in NiO the magnetization of oxygen atoms was found to be exactly zero, as there was a direct exchange between the neighboring nickel atoms.[63]

Addition of on-site exchange terms for copper atoms (DFT+U method) caused the corresponding magnetization to increase up to 0.734 μ_B (its d-orbital population was equal to 8.883 e). The magnetization attributed to the atoms O(1) (0.007), O(2) (0.045), and O(3) (0.037) remained qualitatively (half) the same as obtained from the LSDA calculation. In both cases, the total magnetization was calculated to be zero for a supercell.

On the basis of the results of LSDA and DFT+U calculations, we again may conclude that all the oxygen atoms in a crystal of $Na_2Cu(CO_3)_2$ are involved in the superexchange between the copper centers, including O(1) forming only weak Cu···O interaction. Our data additionally show that p-electrons of the oxygen atoms are responsible for this. As p-electrons of the oxygen atoms in a carbonate moiety are hybridized into σ and π molecular orbitals, the latter finding does not contradict the σ mechanism of superexchange previously proposed for $Na_2Cu(CO_3)_2$.[19]

Topological analysis of the computed (LSDA and DFT+U) electron density distributions gave the same [4 + 2] binding pattern for the copper ion as did the experimental structure factors and multipole expansion, although being devoid of their deficiencies. In all cases, two additional stabilizing interactions Cu···O were found involving the atom O(1) located at 3.6 Å from the transition metal center; other bcps also remained (Table 6). However, these electron densities display the highest values of the corresponding topological parameters among the three approaches used: it overestimated the energy of interatomic interactions in $Na_2Cu(CO_3)_2$ by 0.2−7.9 kcal/mol (the largest value corresponds to the strongest Cu−O(2) bond, the lowest to the Cu···O(1) interaction), although nicely reproducing their relative strength. In particular, both the LSDA and DFT+U calculations assigned the energy of 0.6 kcal/mol for the weak Cu···O(1) binding against 0.4 kcal/mol

dx.doi.org/10.1021/ic4024025 | *Inorg. Chem.* 2013, 52, 14355−14363

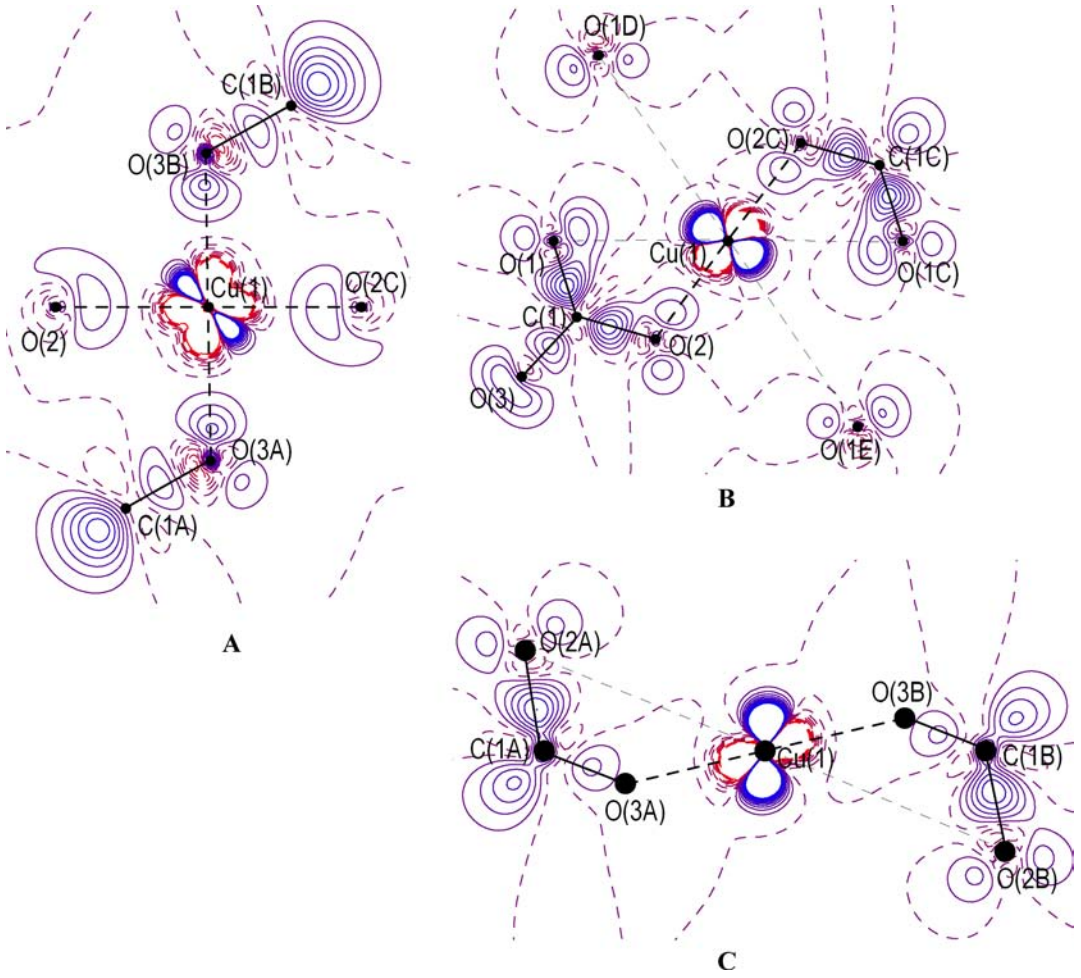

Figure 3. Two-dimensional distribution of the experimental DED in a plane of CuO_4 square (A) and those that are formed by additional contacts Cu···O (B and C) in a crystal of $Na_2Cu(CO_3)_2$. The contours are drawn with a 0.1 eÅ^{-3} step, the negative and zero contours are dashed. For labeling scheme, see caption to Figure 1 and footnote to Table 2.

Table 5. Electronic Population and Magnetization Densities in $Na_2Cu(CO_3)_2$ According to LSDA and DFT+U Periodic Calculations

atom	electronic population (density of states integrated over Wigner–Seitz cells), e				atom	orbital magnetization densities[a] (integrated magnetic moments over the PAW sphere, magnetization), μ_B			
	s	p	d	tot		s	p	d	tot
					LSDA				
Cu(1)	0.249	6.182	8.835	15.266	Cu(1)	−0.003	0.002	−0.581	−0.583
Na(1)	1.936	5.611	0.000	7.547	Na(1)	0.000	0.000	0.000	0.000
O(1)	1.044	2.409	0.000	3.454	O(1)	0.000	0.011	0.000	0.011
O(2)	1.044	2.407	0.000	3.451	O(2)	0.004	0.067	0.000	0.071
O(3)	1.041	2.410	0.000	3.450	O(3)	0.005	0.056	0.000	0.061
C(1)	0.463	0.986	0.000	1.449	C(1)	0.000	0.003	0.000	0.003
					DFT+U				
Cu(1)	0.245	6.184	8.883	15.311	Cu(1)	0.005	0.000	0.728	0.734
Na(1)	1.937	5.611	0.000	7.547	Na(1)	0.000	0.000	0.000	0.000
O(1)	1.043	2.411	0.000	3.454	O(1)	0.000	0.006	0.000	0.007
O(2)	1.041	2.414	0.000	3.455	O(2)	0.003	0.045	0.000	0.048
O(3)	1.039	2.415	0.000	3.455	O(3)	0.004	0.037	0.000	0.042
C(1)	0.463	0.985	0.000	1.448	C(1)	0.000	0.000	0.000	0.000

[a]For each atom, an absolute value of magnetization is given.

obtained from the multipole refinement of experimental or theoretical structure factors.

dx.doi.org/10.1021/ic4024025 | *Inorg. Chem.* 2013, 52, 14355−14363

Table 6. Interatomic Distances and Topological Parameters of $\rho(r)$ in bcps for All the Interionic Interactions in $Na_2Cu(CO_3)_2$ According to LSDA and DFT+U Calculations[a]

interaction	R, Å	$\rho(r)$, eÅ^{-3}	$\nabla^2\rho(r)$, eÅ^{-5}	$-v(r)$, au	$h_e(r)$, au	E_{int}, kcal/mol
Cu(1)−O(2)	1.919	0.71	10.6	0.1752	−0.0279	54.9
Cu(1)−O(3A)	1.942	0.65	10.03	0.1550	−0.0207	48.6
Cu(1)···O(1D)	3.362	0.03	0.34	0.0020	0.0009	0.6
Na(1)−O(2′)	2.342	0.17	3.28	0.0249	0.0061	7.8
Na(1)−O(3″)	2.302	0.15	2.83	0.0204	0.0058	6.4
Na(1)−O(3B)	2.342	0.14	2.62	0.0192	0.0052	6.0
Na(1)−O(1)	2.403	0.13	2.54	0.0177	0.0055	5.5
Na(1)−O(1D)	2.544	0.11	2.21	0.0146	0.0052	4.6
Na(1)−O(1B)	2.544	0.09	1.85	0.0110	0.0050	3.5
O(1)···O(1B)	2.982	0.06	1.00	0.0061	0.0026	1.9
O(3)···O(3‴)	3.194	0.06	1.03	0.0060	0.0028	1.9

[a]All calculations (non-spin-polarized, LSDA and DFT+U) gave the same values of topological parameters.

CONCLUSION

By analyzing electron densities obtained experimentally from X-ray diffraction data, by multipole modeling of theoretical structure factors and from LSDA and DFT+U quantum chemical calculations, we unambiguously showed that in a crystal $Na_2Cu(CO_3)_2$ the copper atom expands its coordination sphere from the accepted square-planar to the elongated tetragonal bipyramide by including two additional oxygen atoms from neighboring $[Cu(CO_3)_2^{2-}]$ layers *via* very weak Cu···O interactions (3.6 Å, 0.5 kcal/mol). These were identified by bcps and bond paths in experimental and theoretical electron densities obtained by multipole expansion as well as computed in quantum chemical calculations. Involving the magnetic orbital of the copper atom, this Cu···O binding is a more probable pathway of antiferromagnetic interaction between the layers than previously suggested possibilities such as a direct exchange between the copper ions and a superexchange *via* sodium atoms. Therefore, the topological analysis does provide the information on the magnetic interactions beyond the presence or the absence of a bcp between the metal centers. Although such a bcp observed with a bridging ligand is not meant to exactly visualize a magnetic interaction in a system, it reveals even the weakest interatomic contacts that may mediate superexchange pathways, thus helping to better understanding magnetic behavior of crystalline solids.

ASSOCIATED CONTENT

Supporting Information

Supplementary figures and an output of the multipole refinement of high-resolution X-ray diffraction data for $Na_2Cu(CO_3)_2$. This material is available free of charge via the Internet at http://pubs.acs.org.

AUTHOR INFORMATION

Corresponding Author

*E-mail: unelya@xrlab.ineos.ac.ru.

Author Contributions

The manuscript was written through contributions of all authors. All authors have given approval to the final version of the manuscript.

Notes

The authors declare no competing financial interest.

ACKNOWLEDGMENTS

This study was financially supported by the Russian Foundation for Basic Research (Projects 13-03-00772 and 12-03-33107), the Foundation of the President of the Russian Federation (Projects MK-6938.2012.3, MK-5181.2013.3, and MD-1020.2012.3), and the Russian Science Support Foundation.

REFERENCES

(1) Kahn, O. *Molecular Magnetism*; Wiley-VCH Verlag GmbH: Weinheim, 1993.
(2) Miller, J. S.; Drillon, M. *Magnetism: Molecules to Materials*; Wiley-VCH Verlag GmbH: Weinheim, 2002.
(3) Itoh, K.; Kinoshita, M. *Molecular Magnetism: New Magnetic Materials*; Gordon and Breach Science Publishers: Amsterdam, 2000.
(4) Pardo, E.; Train, C.; Liu, H.; Chamoreau, L.-M.; Dkhil, B.; Boubekeur, K.; Lloret, F.; Nakatani, K.; Tokoro, H.; Ohkoshi, S.; Verdaguer, M. *Angew. Chem., Int. Ed.* **2012**, *51*, 8356−8360.
(5) Düring, J.; Hölzer, A.; Kolb, U.; Branscheid, R.; Gröhn, F. *Angew. Chem., Int. Ed.* **2013**, DOI: 10.1002/anie.201302773.
(6) Bader, R. F. W. *Atoms in Molecules. A Quantum Theory*; Clarendron Press: Oxford, 1990.
(7) Abramov, Y. A. *Acta Crystallogr., Sect. A* **1997**, *53*, 264−272.
(8) Espinosa, E.; Molins, E.; Lecomte, C. *Chem. Phys. Lett.* **1998**, *285*, 170−173.
(9) Espinosa, E.; Alkorta, I.; Rozas, I.; Elguero, J.; Molins, E. *Chem. Phys. Lett.* **2001**, *336*, 457−461.
(10) Lyssenko, K. A. *Mendeleev Commun.* **2012**, *22* (), 1−7.
(11) Pillet, S.; Souhassou, M.; Mathoniere, C.; Lecomte, C. *J. Am. Chem. Soc.* **2004**, *126*, 1219−1228.
(12) Pillet, S.; Souhassou, M.; Lecomte, C. *Acta Crystallogr., Sect. A* **2004**, *60*, 455−464.
(13) Clausen, H. F.; Overgaard, J.; Chen, Y. S.; Iversen, B. B. *J. Am. Chem. Soc.* **2008**, *130*, 7988−7996.
(14) Farrugia, L. J.; Middlemiss, D. S.; Sillanpaa, R.; Seppala, P. *J. Phys. Chem. A* **2008**, *112*, 9050−9067.
(15) Poulsen, R. D.; Bentien, A.; Graber, T.; Iversen, B. B. *Acta Crystallogr., Sect. A* **2004**, *60*, 382−389.
(16) Bouhmaida, N.; Mendez-Rojas, M. A.; Perez-Benitez, A.; Merino, G.; Fraisse, B.; Ghermani, N. E. *Inorg. Chem.* **2010**, *49*, 6443−6452.
(17) Maslen, E. N.; Spadaccini, N.; Watson, K. J.; White, A. H. *Acta Crystallogr., Sect. B* **1986**, *42*, 430−436.
(18) Schluter, J.; Pohl, D. *Neues Jahrbuch Fur Mineralogie-Abhandlungen* **2005**, *182*, 11−14.
(19) Gregson, A. K.; Moxon, N. T. *Inorg. Chem.* **1981**, *20*, 78−81.
(20) Meskine, H.; Satpathy, S. *Phys. Rev. B* **2005**, *72*, 9.
(21) Escuer, A.; Mautner, F. A.; Penalba, E.; Vicente, R. *Inorg. Chem.* **1998**, *37*, 4190−4196.

(22) Youngme, S.; Chaichit, N.; Kongsaeree, P.; van Albada, G. A.; Reedijk, J. *Inorg. Chim. Acta* **2001**, *324*, 232−240.
(23) SAINT and SADABS computer programs. Bruker AXS, Inc.: Madison, WI, 1999.
(24) Sheldrick, G. M. *Acta Crystallogr., Sect. A* **2008**, *64*, 112−122.
(25) Hansen, N. K.; Coppens, P. *Acta Crystallogr., Sect. A* **1978**, *34*, 909−921.
(26) Volkov, A.; Macchi, P.; Farrugia, L. J.; Gatti, C.; Mallinson, P.; Richter, T.; Koritsanszky, T. *Acta Crystallogr., Sect. A* **2006**, *57*, 656−662.
(27) Su, Z. W.; Coppens, P. *Acta Crystallogr., Sect. A* **1995**, *51*, 27−32.
(28) Hirshfeld, F. L. *Acta Crystallogr., Sect. A* **1976**, *32*, 239−244.
(29) Dovesi, R.; Orlando, R.; Civalieri, B.; Roetti, C.; Saunders, V. R.; Zicovich-Wilson, C. M. *Z. Kristallogr.* **2005**, *220*, 571−573.
(30) Becke, A. D. *J. Chem. Phys.* **1993**, *98*, 5648−5652.
(31) Peintinger, M. F.; Oliveira, D. V.; Bredow, T. *J. Comput. Chem.* **2013**, *34*, 451−459.
(32) Stash, A.; Tsirelson, V. *J. Appl. Crystallogr.* **2002**, *35*, 371−373.
(33) Kirzhnits, D. A. *Sov. Phys.—JETP* **1957**, *5*, 64−72.
(34) Lyssenko, K. A.; Korlyukov, A. A.; Antipin, M. Y. *Mendeleev Commun.* **2005**, *3*, 90−92.
(35) Pidko, E. A.; van Santen, R. A. *ChemPhysChem* **2006**, *7*, 1657−1660.
(36) Pidko, E. A.; Xu, J.; Mojet, B. L.; Lefferts, L.; Subbotina, I. R.; Kazansky, V. B.; van Santen, R. A. *J. Phys. Chem. B* **2006**, *110*, 22618−22627.
(37) Sobczyk, L.; Grabowski, S. J.; Krygowski, T. M. *Chem. Rev.* **2005**, *105*, 3513−3560.
(38) Nelyubina, Y. V.; Lyssenko, K. A. *Chem.—Eur. J.* **2012**, *18*, 12633−12636.
(39) Borissova, A. O.; Korlyukov, A. A.; Antipin, M. Y.; Lyssenko, K. A. *J. Phys. Chem. A* **2008**, *112*, 11519−11522.
(40) Puntus, L. N.; Lyssenko, K. A.; Antipin, M. Y.; Bunzli, J.-C. G. *Inorg. Chem.* **2008**, *47*, 11095−11107.
(41) Lyssenko, K. A.; Korlyukov, A. A.; Golovanov, D. G.; Ketkov, S. Y.; Antipin, M. Y. *J. Phys. Chem. A* **2006**, *110*, 6545−6551.
(42) Glukhov, I. V.; Lyssenko, K. A.; Korlyukov, A. A.; Antipin, M. Y. *Faraday Discuss.* **2007**, *135*, 203−215.
(43) Nelyubina, Y. V.; Glukhov, I. V.; Antipin, M. Y.; Lyssenko, K. A. *Chem. Commun.* **2010**, *46*, 3469−3471.
(44) Kresse, G.; Hafner, J. *Phys. Rev. B* **1993**, *47*, 558−561.
(45) Kresse, G.; Hafner, J. *Phys. Rev. B* **1994**, *49*, 14251−14269.
(46) Kresse, G.; Furthmüller, J. *Comput. Mater. Sci.* **1996**, *6*, 15−60.
(47) Kresse, G.; Furthmüller, J. *Phys. Rev. B* **1996**, *54*, 11169−11186.
(48) Vanderbilt, D. *Phys. Rev. B* **1990**, *41*, 7892−7895.
(49) Kresse, G.; Hafner, J. *J. Phys.: Condens. Matter* **1994**, *6*, 8245.
(50) Perdew, J. P.; Burke, K.; Ernzerhof, M. *Phys. Rev. Lett.* **1996**, *77*, 3865−3868.
(51) Perdew, J. P.; Burke, K.; Ernzerhof, M. *Phys. Rev. Lett.* **1997**, *78*, 1396.
(52) Gonze, X.; Amadon, B.; Anglade, P.-M.; Beuken, J.-M.; Bottin, F.; Boulanger, P.; Bruneval, F.; Caliste, D.; Caracas, R.; Cote, M.; Deutsch, T.; Genovese, L.; Ghosez, P.; Giantomassi, M.; Goedecker, S.; Hamann, D. R.; Hermet, P.; Jollet, F.; Jomard, G.; Leroux, S.; Mancini, M.; Mazevet, S.; Oliveira, M. J. T.; Onida, G.; Pouillon, Y.; Rangel, T.; Rignanese, G.-M.; Sangalli, D.; Shaltaf, R.; Torrent, M.; Verstraete, M. J.; Zerah, G.; Zwanziger, J. W. *Comput. Phys. Commun.* **2009**, *180*, 2582−2615.
(53) Gregson, A. K.; Moxon, N. T. *Inorg. Chem.* **1982**, *21*, 3464−3466.
(54) Cremer, D.; Kraka, E. *Croat. Chim. Acta* **1984**, *57*, 1259−1281.
(55) Overgaard, J.; Hibbs, D. E.; Rentschler, E.; Timco, G. A.; Larsen, F. K. *Inorg. Chem.* **2003**, *42*, 7593−7601.
(56) Overgaard, J.; Larsen, F. K.; Schiott, B.; Iversen, B. B. *J. Am. Chem. Soc.* **2003**, *125*, 11088−11099.
(57) Gibbs, G. V.; Spackman, M. A.; Jayatilaka, D.; Rosso, K. M.; Cox, D. F. *J. Phys. Chem. A* **2006**, *110*, 12259−12266.
(58) Nelyubina, Y. V.; Antipin, M. Y.; Belokoneva, E. L.; Lyssenko, K. A. *Mendeleev Commun.* **2007**, *17*, 71−73.
(59) Jorgensen, M. R. V.; Cenedese, S.; Clausen, H. F.; Overgaard, J.; Chen, Y. S.; Gatti, C.; Iversen, B. B. *Inorg. Chem.* **2013**, *52*, 297−305.
(60) Pendas, A. M.; Francisco, E.; Blanco, M. A.; Gatti, C. *Chem.—Eur. J.* **2007**, *13*, 9362−9371.
(61) Holladay, A.; Leung, P.; Coppens, P. *Acta Crystallogr., Sect. A* **1983**, *39*, 377−387.
(62) Cortes-Guzman, F.; Bader, R. F. W. *Coord. Chem. Rev.* **2005**, *249*, 633−662.
(63) Kwon, S. K.; Min, B. I. *Phys. Rev. B* **2000**, *62*, 73−75.